Published in final edited form as:
J Immunol. 2013 September 15; 191(6): 2999–3005. doi:10.4049/jimmunol.1301483.

Neuromyelitis Optica IgG Causes Placental Inflammation and Fetal Death

Samira Saadoun[*], **Patrick Waters**[†], **M. Isabel Leite**[†], **Jeffrey L. Bennett**[‡,§], **Angela Vincent**[†], and **Marios C. Papadopoulos**[*]

[*]Academic Neurosurgery Unit, St. George's, University of London, London SW17 0RE, United Kingdom

[†]Nuffield Department of Clinical Neurosciences, University of Oxford, Oxford OX3 9DU, United Kingdom

[‡]Department of Neurology, University of Colorado School of Medicine, Aurora, CO 80045

[§]Department of Ophthalmology, University of Colorado Denver, Aurora, CO 80045

Abstract

Neuromyelitis optica (NMO) is an inflammatory demyelinating disease of the CNS and affects women of childbearing age. Most patients with NMO have circulating Abs, termed NMO-IgG, against the astrocytic water channel protein aquaporin-4. In the CNS, NMO-IgG causes complement-mediated astrocyte damage, inflammatory cell infiltration, and myelin loss. In this study, we show that aquaporin-4 is expressed in the syncytiotrophoblast of human and mouse placenta. Placental aquaporin-4 expression is high during mid-gestation and progressively decreases with advancing pregnancy. Intraperitoneally injected NMO-IgG binds mouse placental aquaporin-4, activates coinjected human complement, and causes inflammatory cell infiltration into the placenta and placental necrosis. There was no damage to maternal organs that express aquaporin-4, including the brain, spinal cord, kidneys, and skeletal muscle. In control experiments, no placentitis was found in mice injected with NMO-IgG without complement, non–NMO-IgG with human complement, or in aquaporin-4 null mice injected with NMO-IgG and human complement. The infiltrating cells were primarily neutrophils with a few scattered eosinophils and macrophages. NMO-IgG and human complement–induced placentitis caused fetal death, but some fetuses were born normal when lower amounts of NMO-IgG and human complement were injected. Sivelestat, a neutrophil elastase inhibitor, and aquaporumab, a nonpathogenic IgG that competes with NMO-IgG for aquaporin-4 binding, significantly reduced NMO-IgG and human complement induced placentitis and fetal death. Our data suggest that NMO-IgG can cause miscarriage, thus challenging the concept that NMO affects only the CNS. These findings have implications for the management of NMO during pregnancy.

Address correspondence and reprint requests to: Dr. Marios C. Papadopoulos, Academic Neurosurgery Unit, Room 1.122 Jenner Wing, St. George's, University of London, London SW17 0RE, U.K. mpapadop@sgul.ac.uk.

Disclosures

The authors have no financial conflicts of interest.

Neuromyelitis optica (NMO) is an inflammatory, demyelinating disease of the CNS, with predilection for the optic nerve and spinal cord (1, 2); 68–91% of patients with NMO have circulating IgG_1 Abs against extracellular conformational epitopes of aquaporin-4 (AQP4), termed NMO-IgG (3–5). AQP4, the main water channel protein in the CNS, is expressed in the plasma membrane of astrocytes, primarily the perivascular foot processes and the glia-limiting membrane (6).

The pathophysiology of NMO CNS lesions has been studied extensively in humans (7–9), rodent models (10–13), mouse spinal cord slices (14), and cultured cells (15, 16). These studies revealed that NMO-IgG has a key role in NMO lesion formation. After binding to AQP4, NMO-IgG activates the classical complement pathway, causing deposition of membrane attack complexes (C5b-9) in astrocyte plasma membranes. Astrocytes become damaged, which leads to loss of AQP4 and loss of glial fibrillary acidic protein (GFAP) expression. Inflammatory cells (initially neutrophils with eosinophils and later macrophages) then infiltrate into the lesion, causing oligodendrocyte damage and myelin loss (1).

Female:male ratios range between 3:1 and 10:1, with a mean age at onset 34–43 y (1, 2). Therefore, many patients with NMO are women of childbearing age. The effect of pregnancy on NMO has been studied recently: the risk of acute NMO attacks is elevated in the first trimester postpartum (17, 18). However, the effect of NMO on the placenta and fetus is unclear. In a retrospectively ascertained cohort of patients from the National NMO Service (Oxford, U.K.), 13% of the pregnancies in NMO-IgG^+ women ended in miscarriage. This number rises to 33% if the pregnancies occurring more than 1 y before disease onset are excluded (Leite et al., manuscript in preparation). A case report showed spontaneous miscarriage associated with placental inflammation in a patient with NMO-IgG^+ (19), but others reported normal pregnancies in NMO-IgG^+ women receiving treatment (20). Our aim was to determine whether NMO-IgG damages the fetoplacental unit.

Materials and Methods

Mice

We used CD1 wild type (WT) and AQP4-null (KO) mice (21) that were 8–12 wk old. Protocols were approved by the British Home Office. Investigators analyzing the data were unaware of mouse genotype and type of IgG injected.

Mouse tissue

Anesthetized mice were perfused-fixed through the left cardiac ventricle with 0.9% saline followed by 4% formaldehyde. Tissues were removed and postfixed in 4% formaldehyde, dehydrated, and processed into paraffin. We also purchased ready-to-use CD1 mouse embryonic day (E) 10 to E18 placenta tissue sections (AMS Biotechnology, Abingdon, U.K.). Sections were stained with H&E or immunostained as described.

Human tissue

We used normal human tissue (formalin fixed, paraffin embedded) including fetal brain and spinal cord (20 and 40 wk old; Abcam, Cambridge, U.K.), placenta (15–20 wk; AmsBio, Abingdon, U.K.; GeneTex/TebuBio, Peter-borough, U.K.; Insight Biotechnology, Wembley, U.K.), ovaries, uterus, and cervix (Insight Biotechnology, Wembley, U.K.). Normal 40-wk-old placentas were obtained from the Department of Pathology at St. George's Hospital. Tissue sections were stained with H&E or immunostained for AQP4.

Quantification of staining

We examined four sections for each human placenta and two sections for each mouse placenta.

Baseline placental AQP4 immunoreactivity—We quantified syncytiotrophoblast AQP4 expression as the percentage of 10 high-power fields that were immunopositive: 0, for 0–25%; +, for 25–50%; ++, for 50–75%; +++, for 75–100%.

Placental inflammation (H&E)—We determined the placenta to be inflamed if it had at least one aggregate of extravascular inflammatory cells.

Placental C5b-9 immunoreactivity—We determined the placenta C5b-9 to be immunopositive if it had at least one immunolabeled area.

Placental AQP4 expression after i.p. injection—AQP4 expression was determined to be normal if the grade was ++ or +++. Investigators were unaware of the experimental conditions when examining samples.

NMO-IgG and control IgG

Sera from two patients with NMO (with strong AQP4 autoantibody serum positivity), and two healthy subjects were processed to obtain the IgG fractions, termed IgG_{NMO} and IgG_{CON}, respectively. IgG concentration was 6–38 mg/ml. C_{hu} was collected from healthy volunteers. Details are given elsewhere (12). Purified human monoclonal recombinant NMO-IgGs (rAb-53 and rAb-58) were generated as described, and a measles virus-specific rAb (2B4) was used as isotype-matched control (10). We termed these Abs NMO-IgG_{53}, NMO-IgG_{58}, and CON-IgG_{2B4}. Labeling of NMO-IgG_{58} and CON-IgG_{2B4} with the red fluorophore Cy3 (NMO-IgG_{53}[Cy3], CON-IgG_{2B4}[Cy3]) was done using the Amersham Cy3 Ab Labeling Kit (GE Healthcare, Buckinghamshire, U.K.).

Mouse i.p. IgG and C_{hu} injections

To determine placental inflammation and fetal death, we injected pregnant mice with 0.8 ml polyclonal Ab (IgG_{NMO}) or 25 μg recombinant mAb (NMO-IgG_{53}, NMO-IgG_{58}, CON-IgG_{2B4}) plus 0.8 ml C_{hu}. Pregnant mice were injected at E12, reinjected at E13, and killed at E14. One mouse was injected at E7, reinjected at E8, and killed at E9. To determine binding of NMO-IgG_{53}[CY3] (and CON-IgG_{2B4}[Cy3]) to the placenta, 25 μg was injected i.p., and mice were killed 6 h later. To determine the litter size at birth, mice were injected i.p. with 10 μg NMO-IgG_{53} (or CON-IgG_{2B4}) plus 0.4 ml C_{hu} at E12, E15, and E18.

Sivelestat and aquaporumab

Sivelestat (ONO-5046) was purchased from Tocris Bioscience (Bristol, U.K.). Point mutations were introduced into the IgG_1 Fc sequence of the NMO-IgG_{53} H chain (L234A, L235A) to produce an aquaporumab that lacks effector functions (10, 22). We injected 3 mg sivelestat or 75 μg aquaporumab i.p. (plus 25 μg NMO-IgG_{53} and 0.8 ml C_{hu}) at E12, reinjected at E13, and killed the mice at E14.

Tissue staining

Sections were incubated with primary Ab (1 h, at room temperature or overnight at 4°C) followed by biotinylated secondary Ab (Vector Laboratories, Peterborough, UK) and avidin-linked HRP. Primary Abs were polyclonal rabbit anti-AQP4 (1:100; Millipore, Livingstone, U.K.), polyclonal rabbit anti–C5b-9 (1:100; Abcam, Cambridge, U.K.), polyclonal rat 1A8 anti Ly6G for neutrophils (1:100; BD Biosciences, Oxford, U.K.), polyclonal rat anti-macrophage (1:100; eBioscience, Hatfield, U.K.), polyclonal rabbit anti-CD3 (1:500; Dako Cytomation, Ely, U.K.). Immunostaining was visualized brown using DAB/H_2O_2. Counterstaining was with performed hematoxylin. Some human placentas were immunostained for AQP4 followed by AlexaFluor-labeled secondary Ab. Eosinophils were visualized fluorescent red after tissue staining using the Eoprobe kit (SurModics, Edina, MN).

In vivo AQP4 labeling of mouse placenta

E12 pregnant mice were injected i.p. with 25 μg NMO-IgG_{53}[Cy3] or CON-IgG_{2B4}[Cy3] and killed 6 h after. The placentas were removed, fixed in paraformaldehyde for 1 h at room temperature, dehydrated in 30% sucrose overnight, and embedded in OCT. Tissue sections (7 μm) were incubated with polyclonal rabbit anti-AQP4 (1:100; Millipore) followed by FITC-anti-rabbit secondary Ab (1:200, Vector Labs, Peterborough, U.K.). Nuclei were labeled blue with DAPI.

Statistics

Two groups were compared with two-tailed Student *t* test using Microsoft Excel for Mac 2011 (version 14.3.2). Data in Fig. 4 (sivelestat, aquaporumab) were compared with one-way ANOVA and posthoc Tukey test at www.vassarstats.net.

Results

AQP4 expression in human female reproductive organs

No AQP4 was found in the human ovary including stroma, cortex, follicles (Fig. 1A) or uterus including endometrium, myometrium, perimetrium, and cervix (Fig. 1B). AQP4 was strongly expressed in human placental syncytiotrophoblast obtained from the second trimester of pregnancy, with little or no AQP4 expression in the third trimester (Fig. 1C). There was no AQP4 in the placental stroma or endothelium. Immunofluorescence staining suggested plasma membrane AQP4 expression in the syncytiotrophoblast.

AQP4 expression in mouse female reproductive organs

No AQP4 was found in the mouse ovary or uterus (Fig. 1D, 1E). Mouse placental syncytiotrophoblast began to express AQP4 at E11, reaching maximal level at E13, with progressively reduced AQP4 immunoreactivity until birth (Fig. 1F). AQP4 immunostaining was in a wire-loop pattern, characteristic of the syncytiotrophoblast plasma membrane. There was no AQP4 in the placenta of E13 KO mice. Therefore, AQP4 expression in the female mouse reproductive tract is comparable with human.

NMO-IgG binds placental AQP4 in vivo

Cy3-tagged, AQP4-specific, recombinant monoclonal NMO-IgG (NMO-IgG_{58}[Cy3]) or isotype recombinant IgG control (CON-IgG_{2B4}[Cy3]) was injected i.p. in E12 pregnant mice. At 6 h, NMO-IgG_{58}[Cy3] labeled the syncytiotrophoblast (Fig. 1G). In double labeling experiments, NMO-IgG_{58}[Cy3] colocalized with commercial FITC-tagged anti-AQP4 Ab. There was no syncytiotrophoblast labeling when CON-IgG_{2B4}[Cy3] was injected or in KO mice injected with NMO-IgG_{58}[Cy3]. Therefore, circulating NMO-IgG enters the placenta and binds placental AQP4.

NMO-IgG causes placental inflammation

In these experiments, C_{hu} was coinjected with NMO-IgG because NMO-IgG does not activate mouse complement (12). We observed inflammatory cell infiltration into E14 placenta, after i.p. injections at E12 and E13 of NMO-IgG_{58} plus C_{hu} or the IgG fraction from NMO patient serum (IgG_{NMO}) plus C_{hu} (Fig. 2A, 2B). C5b-9 was deposited widely, and AQP4 expression was lost in the inflamed placentas. Some placentas had marked leukocyte infiltration and necrotic areas (Fig. 2C). Most of the infiltrating leukocytes were neutrophils with a few scattered eosinophils and macrophages, but no T lymphocytes (Fig. 2D). In control experiments, no leukocyte infiltration, no C5b-9 immunoreactivity, and no loss of AQP4 expression were found in placentas after injecting i.p. CON-IgG_{2B4} plus C_{hu}, IgG from healthy individuals (IgG_{CON}) plus C_{hu} or NMO-IgG_{58} (without C_{hu}). There was no placental leukocyte infiltration and no C5b-9 immunoreactivity after injecting i.p. NMO-IgG_{58} plus C_{hu} in KO mice. There was no placental inflammation in an E9 pregnant mouse that had i.p. injections of NMO-IgG_{58} plus C_{hu} at E7 and E8—that is, at gestational stages without placental AQP4 expression (Fig. 2E). The results of these experiments suggest that after binding the syncytiotrophoblast, NMO-IgG causes C_{hu} activation, loss of AQP4 expression, and placental leukocyte infiltration.

Although circulating NMO-IgG also binds AQP4 in other organs including kidney and skeletal muscle (23), there was no inflammatory cell infiltration or loss of AQP4 expression in the brains, spinal cords, kidneys, or skeletal muscles of the injected mice (Fig. 2F). Therefore, i.p. injected NMO-IgG and C_{hu} selectively damage the placenta sparing other AQP4 expressing organs.

NMO-IgG–induced placentitis causes fetal death

We counted the number of dead fetuses (in utero and spontaneously aborted) at E14 after injecting (at E12 and E13) NMO-IgG_{58} plus C_{hu} or IgG_{NMO} plus C_{hu} or CON-IgG_{2B4} plus C_{hu} or NMO-IgG_{58} (without C_{hu}) in WT mice or NMO-IgG_{58} plus C_{hu} in KO mice (Fig.

3A, 3B). There were significantly more dead fetuses in WT mice after injecting NMO-IgG_{58} (or IgG_{NMO}) plus C_{hu} versus CON-IgG_{2B4} (or IgG_{CON}) plus C_{hu}. There were no dead fetuses after injecting NMO-IgG_{58} (without C_{hu}) and only one dead fetus after injecting NMO-IgG_{58} plus C_{hu} in KO mice. Pregnant mice, which received a low dose of another AQP4-specific, recombinant monoclonal NMO-IgG (NMO-IgG_{53}) plus C_{hu} every 2 d starting at E12, delivered significantly fewer pups than did pregnant mice similarly injected with CON-IgG_{2B4} plus C_{hu} or noninjected mice (Fig. 3C). The pups from the mice injected with NMO-IgG_{53} plus C_{hu} appeared normal (Fig. 3D) and had histologically normal brains, spinal cords, kidneys, and skeletal muscles (Fig. 3E). Therefore, NMO-IgG–induced placentitis causes fetal death, but some fetuses are born normal when NMO-IgG levels are lower.

AQP4 is expressed in human fetal CNS

There was strong AQP4 expression in the frontal lobes and spinal cords of two human fetuses aged 20 and 40 wk (Fig. 3F). As in adult CNS, the fetal AQP4 was located perivascularly and in the glia limiting membrane in the brain and spinal cord. No AQP4 was found in the brain or spinal cord of E14 and E18 fetal mice (not shown).

Sivelestat and aquaporumab reduce NMO-IgG-induced placentitis

We tested whether two emerging NMO treatments, sivelestat and aquaporumab, reduce placentitis and fetal death induced by NMO-IgG plus C_{hu} (Fig. 4). Sivelestat is a selective neutrophil elastase inhibitor that inhibits neutrophil infiltration into mouse brain NMO lesions (24). Aquaporumab is a recombinant monoclonal NMO-IgG that lacks effector functions and sterically hinders pathogenic NMO-IgG from binding AQP4, thus reducing brain NMO lesions in mice (22). Sivelestat did not inhibit NMO-IgG_{53}–induced C_{hu} activation or loss of AQP4 expression in the placenta. Although C_{hu}-mediated damage to the syncytiotrophoblast was not inhibited, sivelestat markedly reduced placental neutrophil infiltration and fetal death. Aquaporumab inhibited the NMO-IgG_{53}–induced C_{hu} activation, loss of placental AQP4 expression and the placental neutrophil infiltration and fetal death.

Discussion

We showed that NMO-IgG can damage the mouse placenta and cause fetal death. Three factors (NMO-IgG, AQP4, and C_{hu}) are required for the placental inflammation to occur. Excluding any one of these factors (using CON-IgG instead of NMO-IgG, using a KO mouse instead of WT, omitting C_{hu}) does not produce placental inflammation. These findings might explain the placental inflammation, complement activation in the syncytiotrophoblast, loss of AQP4 expression, and miscarriage in an NMO-IgG^+ pregnant patient, which occurred at 21 wk (when placental AQP4 expression is high) (19). Our data might also account for the increased risk of miscarriage in NMO-IgG^+ women (Leite et al., manuscript in preparation). It would be interesting to investigate the risk of miscarriage in seronegative NMO patients and in NMO-IgG^+ patients who do not meet all clinical criteria for NMO (25). Because NMO-IgG is essential for placental inflammation and fetal death to occur, we predict that the risk of miscarriage is not elevated in seronegative NMO patients, but is high in NMO-IgG^+ patients. Our data suggest that, to prevent miscarriage, NMO-IgG

levels should be monitored during pregnancy and kept low. However, in some patients with NMO, autoantibodies other than NMO-IgG (26, 27) might also have a role in pregnancy-related complications.

Based on our findings, we propose the following mechanism for NMO-IgG–mediated placental damage (summarized in Fig. 5). NMO-IgG binds the placental syncytiotrophoblast of fetal villi and activates the classical complement pathway. C5b-9 becomes deposited in the syncytiotrophoblast plasma membrane, thus damaging the syncytiotrophoblast and causing loss of AQP4 expression. Leukocytes (primarily neutrophils) then infiltrate into the placenta, releasing elastase and other proteases that cause further placental damage. Some histologic features of the placental NMO lesions (loss of AQP4 expression, C5b-9 deposition at sites of AQP4 expression, leukocyte infiltration) are analogous to the CNS NMO lesions. Severely inflamed placentas become necrotic, which causes fetal death or spontaneous miscarriage. Less inflamed placentas (as seen when less NMO-IgG and C_{hu} is injected) are compatible with normal fetal survival and birth. The mechanism proposed in this study might explain why some NMO-IgG$^+$ women miscarry, but others have successful, healthy pregnancies.

Little or no AQP4 expression was detected in the human and mouse female reproductive tracts, which is consistent with previous studies that reported little or no AQP4 protein in the human vagina (28) and ovary (29). There is also no AQP4 in human testes and sperm (not shown). The lack of AQP4 expression in the female reproductive tract and sperm suggests that NMO-IgG does not impair the early stages of conception (ovulation, sperm migration, fertilization, and implantation). Our finding of high AQP4 expression in human and mouse placental syncytiotrophoblast, with progressive downregulation throughout pregnancy, is consistent with a previous study (30). The time course of placental AQP4 expression suggests that the placental vulnerability to NMO-IgG–mediated damage is high in the second trimester and decreases as the pregnancy progresses.

AQP4 is one of several aquaporins expressed in the placenta (31). The function of AQP4 and other aquaporins in the placenta during normal pregnancy is unknown. We previously reported that KO×KO mouse matings produce normal pups and normal litter size with normal male:female ratio (32), which suggests that placental AQP4 has only a minor role in normal gestation in mice.

We showed that AQP4 is expressed in human fetal CNS as early as 20 wk, consistent with an earlier report (33). AQP4 in the human fetus is found perivascularly and in the glia limitans, as in human adults. Little or no AQP4 was seen in the brain or spinal cord of fetal mice (not shown), in agreement with rat studies (34). These observations are consistent with the fact that human brains are more developed in utero compared with rodents (35). For example, the brains of 20- and 40-wk-old human embryos correspond developmentally to the brains of mice aged 21 and 30 d after coitus, respectively (36). The lack of AQP4 expression in rodent fetal CNS suggests that fetal death after NMO-IgG and C_{hu} injection is not a direct effect of NMO-IgG on the fetal CNS. However, the presence of AQP4 in human fetal CNS raises the possibility that maternal NMO-IgG might directly damage the human fetal CNS.

Systemically injected NMO-IgG binds AQP4 in peripheral organs (including kidney, skeletal muscle, and stomach), but not in the CNS apart from the area postrema (23). Mice injected i.p. with NMO-IgG and C_{hu} have placental inflammation without CNS or peripheral organ inflammation. There is no CNS inflammation probably because the blood-brain barrier inhibits entry of circulating NMO-IgG and C_{hu} into the CNS. Possible explanations for the lack of inflammation in peripheral organs (other than placenta) include low AQP4 expression, only little C_{hu} reaching these organs, high complement regulator expression, and unique interstitial environments (e.g., high renal osmolality, gastric acidity) that might preclude C_{hu} activation.

We provided proof-of principle that sivelestat (24) and aquaporumab (22) reduce the risk of NMO-IgG–induced miscarriage. The therapeutic efficacy of sivelestat in mice suggests that, after injection with NMO-IgG plus C_{hu}, fetal death is caused by the placental neutrophil infiltration rather than the C_{hu} activation. Trophoblast regeneration (37, 38) might explain why C_{hu} activation damages the syncytiotrophoblast, but does not cause fetal death. Sivelestat has no adverse effects on fetal development and maternal health in rats (39) and humans (40), and it is licensed for clinical use in Japan. Aquaporumab has not been tested in humans, but its NMO-IgG–specific therapeutic mechanism suggests fewer side effects than broad immunosuppression. Provided clinical studies confirm that NMO-IgG causes placental inflammation and fetal death, then sivelestat and aquaporumab may be future treatments for NMO-IgG–induced placentitis. Because sivelestat does not inhibit C_{hu}-mediated damage to the syncytiotrophoblast, it could be part of a therapeutic mixture.

To conclude, we showed that NMO-IgG can cause miscarriage by binding placental AQP4, activating complement, and causing inflammatory cell infiltration. These observations might explain the increased frequency of miscarriages in pregnant patients who are NMO-IgG^+. Our findings also expand the clinical spectrum of AQP4 autoimmunity outside the CNS.

Acknowledgments

This work was supported by a research grant from the Guthy Jackson Charitable Foundation (to M.C.P.); the National Institute for Health Research Oxford Biomedical Research Centre (to P.W. and A.V.); the National Health Service Specialised Services for Neuromyelitis Optica (to P.W., A.V., and M.I.L.); and Guthy-Jackson Charitable Foundation and the National Institutes of Health Grant EY022936 (to J.L.B.).

We thank Dr. L. Bridges at St. George's, University of London for providing human tissue.

Abbreviations used in this article

AQP4	aquaporin-4
C5b-9	complement membrane attack complex
C_{hu}	human complement
CON-IgG_{2B4}	measles virus–specific recombinant IgG1
CON-IgG_{2B4}[Cy3]	Cy3 labeled CON-IgG_{2B4}
E	embryonic day

IgG_{CON}	serum IgG fraction from healthy volunteers
IgG_{NMO}	serum IgG fraction from NMO-IgG+ patients
KO	AQP4 null
NMO	neuromyelitis optica
NMO-IgG_{53}	rAb-53 monoclonal recombinant anti-AQP4 IgG_1
NMO-IgG_{58}	rAb-58 monoclonal recombinant anti-AQP4 IgG_1
NMO-IgG_{53}[Cy3]	Cy3-labeled NMO-IgG_{53}
WT	wild type

References

1. Papadopoulos MC, Verkman AS. Aquaporin 4 and neuromyelitis optica. Lancet Neurol. 2012; 11:535–544. [PubMed: 22608667]
2. Jacob A, McKeon A, Nakashima I, Sato DK, Elsone L, Fujihara K, de Seze J. Current concept of neuromyelitis optica (NMO) and NMO spectrum disorders. J Neurol Neurosurg Psychiatry. 2013; 84:922–930. [PubMed: 23142960]
3. Waters PJ, McKeon A, Leite MI, Rajasekharan S, Lennon VA, Villalobos A, Palace J, Mandrekar JN, Vincent A, Bar-Or A, Pittock SJ. Serologic diagnosis of NMO: a multicenter comparison of aquaporin-4-IgG assays. Neurology. 2012; 78:665–671. discussion 669. [PubMed: 22302543]
4. Lennon VA, Kryzer TJ, Pittock SJ, Verkman AS, Hinson SR. IgG marker of optic-spinal multiple sclerosis binds to the aquaporin-4 water channel. J Exp Med. 2005; 202:473–477. [PubMed: 16087714]
5. Lennon VA, Wingerchuk DM, Kryzer TJ, Pittock SJ, Lucchinetti CF, Fujihara K, Nakashima I, Weinshenker BG. A serum autoantibody marker of neuromyelitis optica: distinction from multiple sclerosis. Lancet. 2004; 364:2106–2112. [PubMed: 15589308]
6. Papadopoulos MC, Verkman AS. Aquaporin water channels in the nervous system. Nat Rev Neurosci. 2013; 14:265–277. [PubMed: 23481483]
7. Lucchinetti CF, Mandler RN, McGavern D, Bruck W, Gleich G, Ransohoff RM, Trebst C, Weinshenker B, Wingerchuk D, Parisi JE, Lassmann H. A role for humoral mechanisms in the pathogenesis of Devic's neuromyelitis optica. Brain. 2002; 125:1450–1461. [PubMed: 12076996]
8. Misu T, Fujihara K, Kakita A, Konno H, Nakamura M, Watanabe S, Takahashi T, Nakashima I, Takahashi H, Itoyama Y. Loss of aquaporin 4 in lesions of neuromyelitis optica: distinction from multiple sclerosis. Brain. 2007; 130:1224–1234. [PubMed: 17405762]
9. Roemer SF, Parisi JE, Lennon VA, Benarroch EE, Lassmann H, Bruck W, Mandler RN, Weinshenker BG, Pittock SJ, Wingerchuk DM, Lucchinetti CF. Pattern-specific loss of aquaporin-4 immunoreactivity distinguishes neuromyelitis optica from multiple sclerosis. Brain. 2007; 130:1194–1205. [PubMed: 17282996]
10. Bennett JL, Lam C, Kalluri SR, Saikali P, Bautista K, Dupree C, Glogowska M, Case D, Antel JP, Owens GP, et al. Intrathecal pathogenic anti-aquaporin-4 antibodies in early neuromyelitis optica. Ann Neurol. 2009; 66:617–629. [PubMed: 19938104]
11. Bradl M, Misu T, Takahashi T, Watanabe M, Mader S, Reindl M, Adzemovic M, Bauer J, Berger T, Fujihara K, et al. Neuromyelitis optica: pathogenicity of patient immunoglobulin in vivo. Ann Neurol. 2009; 66:630–643. [PubMed: 19937948]
12. Saadoun S, Waters P, Bell BA, Vincent A, Verkman AS, Papadopoulos MC. Intra-cerebral injection of neuromyelitis optica immunoglobulin G and human complement produces neuromyelitis optica lesions in mice. Brain. 2010; 133:349–361. [PubMed: 20047900]
13. Zhang H, Verkman AS. Eosinophil pathogenicity mechanisms and therapeutics in neuromyelitis optica. J Clin Invest. 2013; 123:2306–2316. [PubMed: 23563310]

14. Zhang H, Bennett JL, Verkman AS. Ex vivo spinal cord slice model of neuromyelitis optica reveals novel immunopathogenic mechanisms. Ann Neurol. 2011; 70:943–954. [PubMed: 22069219]
15. Hinson SR, Pittock SJ, Lucchinetti CF, Roemer SF, Fryer JP, Kryzer TJ, Lennon VA. Pathogenic potential of IgG binding to water channel extracellular domain in neuromyelitis optica. Neurology. 2007; 69:2221–2231. [PubMed: 17928579]
16. Vincent T, Saikali P, Cayrol R, Roth AD, Bar-Or A, Prat A, Antel JP. Functional consequences of neuromyelitis optica-IgG astrocyte interactions on blood-brain barrier permeability and granulocyte recruitment. J Immunol. 2008; 181:5730–5737. [PubMed: 18832732]
17. Kim W, Kim SH, Nakashima I, Takai Y, Fujihara K, Leite MI, Kitley J, Palace J, Santos E, Coutinho E, et al. Influence of pregnancy on neuromyelitis optica spectrum disorder. Neurology. 2012; 78:1264–1267. [PubMed: 22491862]
18. Bourre B, Marignier R, Zéphir H, Papeix C, Brassat D, Castelnovo G, Collongues N, Vukusic S, Labauge P, Outteryck O, et al. NOMADMUS Study Group. Neuromyelitis optica and pregnancy. Neurology. 2012; 78:875–879. [PubMed: 22402855]
19. Reuss R, Rommer PS, Brück W, Paul F, Bolz M, Jarius S, Boettcher T, Grossmann A, Bock A, Zipp F, et al. A woman with acute myelopathy in pregnancy: case outcome. BMJ. 2009; 339:b4026. [PubMed: 20007656]
20. Pellkofer HL, Suessmair C, Schulze A, Hohlfeld R, Kuempfel T. Course of neuromyelitis optica during inadvertent pregnancy in a patient treated with rituximab. Mult Scler. 2009; 15:1006–1008. [PubMed: 19667025]
21. Ma T, Yang B, Gillespie A, Carlson EJ, Epstein CJ, Verkman AS. Generation and phenotype of a transgenic knockout mouse lacking the mercurial-insensitive water channel aquaporin-4. J Clin Invest. 1997; 100:957–962. [PubMed: 9276712]
22. Tradtrantip L, Zhang H, Saadoun S, Phuan PW, Lam C, Papadopoulos MC, Bennett JL, Verkman AS. Anti-aquaporin-4 monoclonal antibody blocker therapy for neuromyelitis optica. Ann Neurol. 2012; 71:314–322. [PubMed: 22271321]
23. Ratelade J, Bennett JL, Verkman AS. Intravenous neuromyelitis optica autoantibody in mice targets aquaporin-4 in peripheral organs and area postrema. PLoS ONE. 2011; 6:e27412. [PubMed: 22076159]
24. Saadoun S, Waters P, MacDonald C, Bell BA, Vincent A, Verkman AS, Papadopoulos MC. Neutrophil protease inhibition reduces neuromyelitis optica-immunoglobulin G-induced damage in mouse brain. Ann Neurol. 2012; 71:323–333. [PubMed: 22374891]
25. Wingerchuk DM V, Lennon A, Pittock SJ, Lucchinetti CF, Weinshenker BG. Revised diagnostic criteria for neuromyelitis optica. Neurology. 2006; 66:1485–1489. [PubMed: 16717206]
26. Leite MI, Coutinho E, Lana-Peixoto M, Apostolos S, Waters P, Sato D, Melamud L, Marta M, Graham A, Spillane J, et al. Myasthenia gravis and neuromyelitis optica spectrum disorder: a multicenter study of 16 patients. Neurology. 2012; 78:1601–1607. [PubMed: 22551731]
27. Sellner J, Kalluri SR, Cepok S, Hemmer B, Berthele A. Thyroid antibodies in aquaporin-4 antibody positive central nervous system autoimmunity and multiple sclerosis. Clin Endocrinol (Oxf). 2011; 75:271–272. [PubMed: 21521293]
28. Kim SO, Oh KJ, Lee HS, Ahn K, Kim SW, Park K. Expression of aquaporin water channels in the vagina in premenopausal women. J Sex Med. 2011; 8:1925–1930. [PubMed: 21492408]
29. Thoroddsen A, Dahm-Kähler P, Lind AK, Weijdegård B, Lindenthal B, Müller J, Brännström M. The water permeability channels aquaporins 1–4 are differentially expressed in granulosa and theca cells of the preovulatory follicle during precise stages of human ovulation. J Clin Endocrinol Metab. 2011; 96:1021–1028. [PubMed: 21252246]
30. De Falco M, Cobellis L, Torella M, Acone G, Varano L, Sellitti A, Ragucci A, Coppola G, Cassandro R, Laforgia V, et al. Down-regulation of aquaporin 4 in human placenta throughout pregnancy. In Vivo. 2007; 21:813–817. [PubMed: 18019416]
31. Damiano AE. Review: Water channel proteins in the human placenta and fetal membranes. Placenta. 2011; 32(Suppl 2):S207–S211. [PubMed: 21208655]

32. Saadoun S, Tait MJ, Reza A, Davies DC, Bell BA, Verkman AS, Papadopoulos MC. AQP4 gene deletion in mice does not alter blood-brain barrier integrity or brain morphology. Neuroscience. 2009; 161:764–772. [PubMed: 19345723]
33. Gömöri E, Pál J, Abrahám H, Vajda Z, Sulyok E, Seress L, Dóczi T. Fetal development of membrane water channel proteins aquaporin-1 and aquaporin-4 in the human brain. Int J Dev Neurosci. 2006; 24:295–305. [PubMed: 16814974]
34. Wen H, Nagelhus EA, Amiry-Moghaddam M, Agre P, Ottersen OP, Nielsen S. Ontogeny of water transport in rat brain: postnatal expression of the aquaporin-4 water channel. Eur J Neurosci. 1999; 11:935–945. [PubMed: 10103087]
35. Clancy B, Finlay BL, Darlington RB, Anand KJ. Extrapolating brain development from experimental species to humans. Neurotoxicology. 2007; 28:931–937. [PubMed: 17368774]
36. Workman AD, Charvet CJ, Clancy B, Darlington RB, Finlay BL. Modeling transformations of neurodevelopmental sequences across mammalian species. J Neurosci. 2013; 33:7368–7383. [PubMed: 23616543]
37. Watson AL, Burton GJ. A microscopical study of wound repair in the human placenta. Microsc Res Tech. 1998; 42:351–368. [PubMed: 9766430]
38. Mayhew TM. Villous trophoblast of human placenta: a coherent view of its turnover, repair and contributions to villous development and maturation. Histol Histopathol. 2001; 16:1213–1224. [PubMed: 11642741]
39. Nishimura T, Chihara N, Shirakawa R, Sugai S, Sakamoto T, Nakagawa Y, Aze Y, Shimouchi K, Ozeki Y, Fujita T. Reproductive and developmental toxicity studies of landiolol hydrochloride (ONO-1101) (4). Perinatal and postnatal study in rats. J Toxicol Sci. 1997; 22(Suppl 3):537–557. [PubMed: 9483480]
40. Nakajima Y, Masaoka N. Initial experience using Sivelestat to manage preterm labor with a bulging fetal membrane in pregnant women. J Perinatol. 2012; 32:466–468. [PubMed: 22643291]

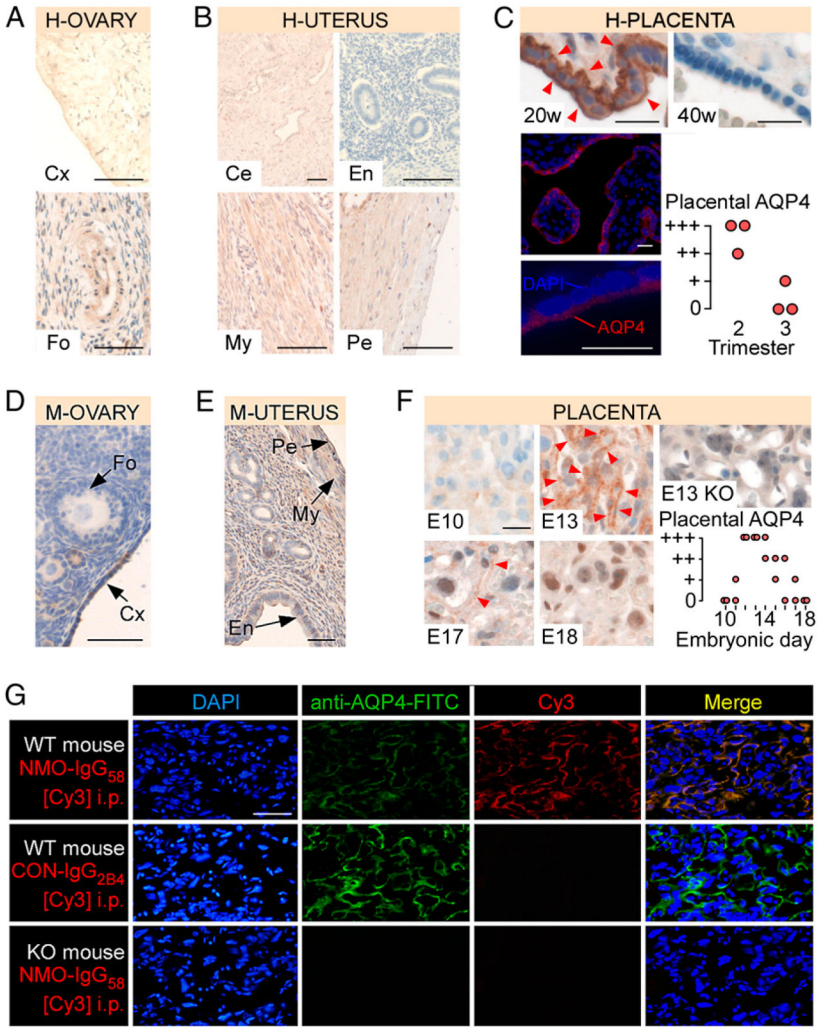

FIGURE 1.

AQP4 is expressed in human and mouse placenta. AQP4 immunoreactivity in (**A**) human ovary (H-OVARY), (**B**) human uterus (H-UTERUS), and (**C**) human placenta (*top*; H-PLACENTA; 20 and 40 wk gestation), AQP4 immunofluorescence in 20 wk human placenta (*bottom left*), and human placental AQP4 versus gestational age (*bottom right*). AQP4 immunoreactivity in (**D**) mouse ovary (M-OVARY), (**E**) mouse uterus (M-UTERUS), (**F**) mouse placenta (*left*; M-PLACENTA; E10, E13, E17, and E18). KO is AQP4 null mouse. Red arrowheads show AQP4. Mouse placental AQP4 versus gestational age is shown (*right*). (**G**) Binding of i.p. injected NMO-IgG_{58}[Cy3] or CON-IgG_{2B4}[Cy3] to placenta (WT or KO mouse). Tissue was double-stained (FITC) with commercial anti-AQP4: blue (DAPI), green (FITC), red (Cy3), and yellow (Merge). Scale bars, 20 μm (C, F), 50 μm (A, D, E, G), and 100 μm (B). Ce, Cervix; Cx, cortex; En, endometrium; Fo, follicle; My, myometrium; Pe, perimetrium.

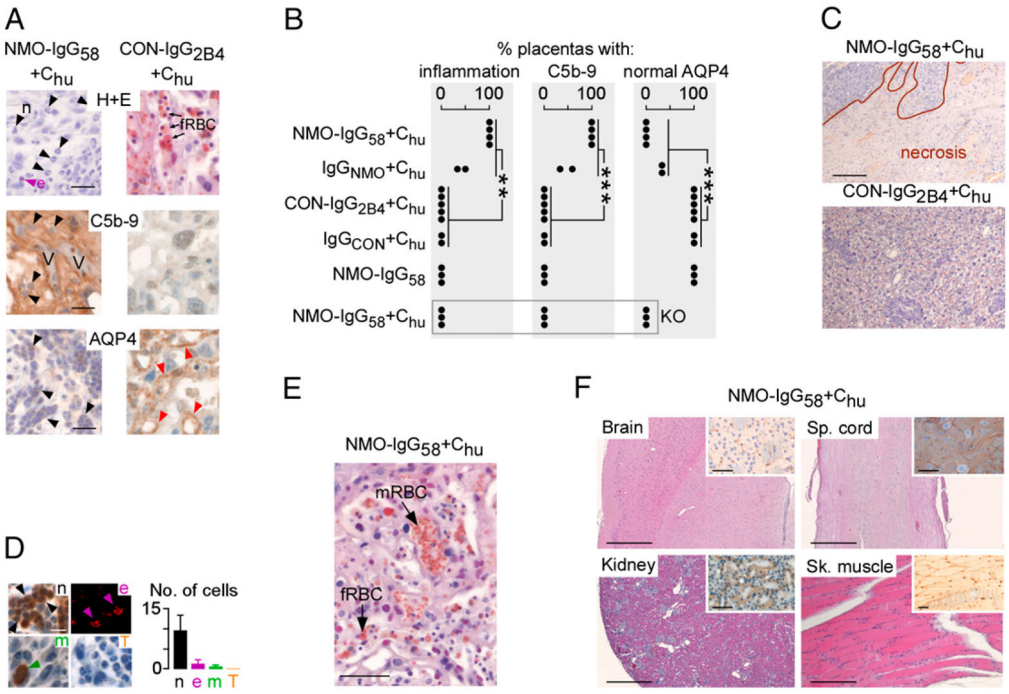

FIGURE 2.

NMO-IgG causes complement-mediated placental inflammation in mice. WT pregnant mice were injected i.p. at E12 and reinjected at E13 with NMO-IgG_{58} plus C_{hu} (n = 4), IgG_{NMO} plus C_{hu} (n = 2), CON-IgG_{2B4} plus C_{hu} (n = 5), IgG_{CON} plus C_{hu} (n = 2) or NMO-IgG_{58} (n = 3) and killed at E14. KO pregnant mice were similarly injected with NMO-IgG_{58} plus C_{hu} (n = 3). (**A**) E14 placentas stained with H&E (*top*), and immunostained for C5b-9 (*middle*) and AQP4 (*bottom*). Neutrophils are indicated by black arrowheads; eosinophil is indicated by a purple arrowhead; AQP4 is indicated by red arrowheads. (**B**) Percent of placentas with (*left*) inflammation, (*middle*) C5b-9 immunoreactivity, and (*right*) normal AQP4 immunoreactivity. Each dot is a pregnant mouse. (**C**) E14 placentas (H&E). (**D**) Inflammatory cells within placental lesions; neutrophils (n, black arrowheads), eosinophils (e, purple arrowheads), macrophages (m, green arrowheads), and T lymphocytes (T). (**E**) A WT pregnant mouse was injected with NMO-IgG_{58} plus C_{hu} at E7, reinjected at E8, and killed at E9. E9 placenta is stained with H&E. (**F**) Brain, spinal cord, kidney, and skeletal muscle from a pregnant mother. *Insets* show H&E and AQP4 immunostain. Scale bars, 10 μm (D), 20 μm (A), 50 μm [(E, F), *insets*], 200 μm [(C, F), sk. Muscle], 500 μm [(F), brain, sp. Cord, kidney]. fRBC, Fetal RBC; mRBC, maternal RBCs.$^{**}p < 0.01$, $^{***}p < 0.001$.

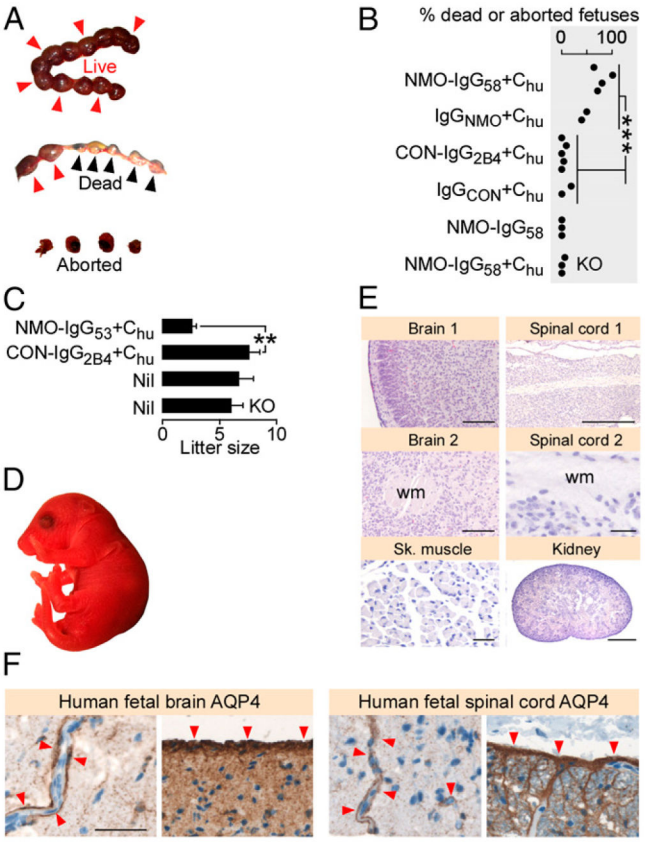

FIGURE 3.

NMO-IgG causes complement-mediated fetal death in mice. (**A**) Live (red arrowheads), dead in utero plus spontaneously aborted (blue arrowheads) fetuses. (**B**) Dead (in utero plus spontaneously aborted) fetuses per pregnant mouse after injection of NMO-IgG_{58} plus C_{hu} (n = 4), IgG_{NMO} plus C_{hu} (n = 2), CON-IgG_{2B4} plus C_{hu} (n = 5), IgG_{CON} plus C_{hu} (n = 2), CON-IgG_{58} (n = 3), or NMO-IgG_{58} plus C_{hu} in KO mice (n = 3). Each dot is a pregnant mouse. (**C**) Litter size delivered after injection of NMO-IgG_{53} plus C_{hu} (n = 3) or CON-IgG_{2B4} plus C_{hu} (n = 5), or without injection (Nil) in WT (n = 7) and KO (n = 5) mice. (**D**) Macroscopic appearance and (**E**) H&E staining of sections of brain, spinal cord, skeletal muscle, and kidney of P1 mouse from a mother that received i.p. NMO-IgG_{53} plus C_{hu}. (**F**) AQP4 immunoreactivity (red arrowheads) in human fetal (*left*) frontal lobe and (*right*) spinal cord. Scale bars, 30 μm [(E) Sp. Cord 2, Sk. Muscle, (F)], 100 mm [(E), brain 1, brain 2], 500 μm [(E) kidney, Sp. Cord 1]. wm, White matter. $^{**}p < 0.01$, $^{***}p < 0.001$.

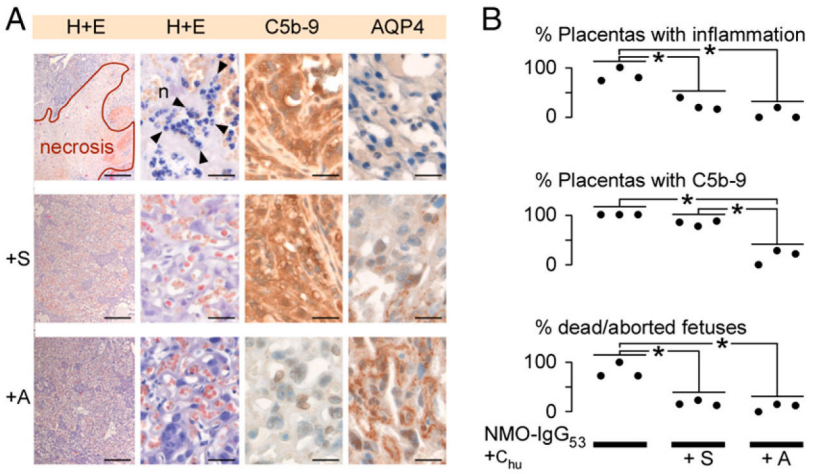

FIGURE 4.

Sivelestat and aquaporumab reduce NMO-IgG–mediated placental damage. (**A**) Placentas (H&E, C5b-9 immunostain, AQP4 immunostain) after i.p. injection of NMO-IgG_{53} plus C_{hu} (n = 3), NMO-IgG_{53} plus C_{hu} plus sivelestat (+S, n = 3) or NMO-IgG_{53} plus C_{hu} plus aquaporumab (+A, n = 3). (**B**) Percentage of placentas with neutrophil infiltration and C5b-9 deposits and percentage of dead fetuses per pregnant mouse. Scale bars, 30 μm [(A) H&E *right*, C5b-9, AQP4], 300 μm [(A) H&E *left*]. *$p < 0.01$.

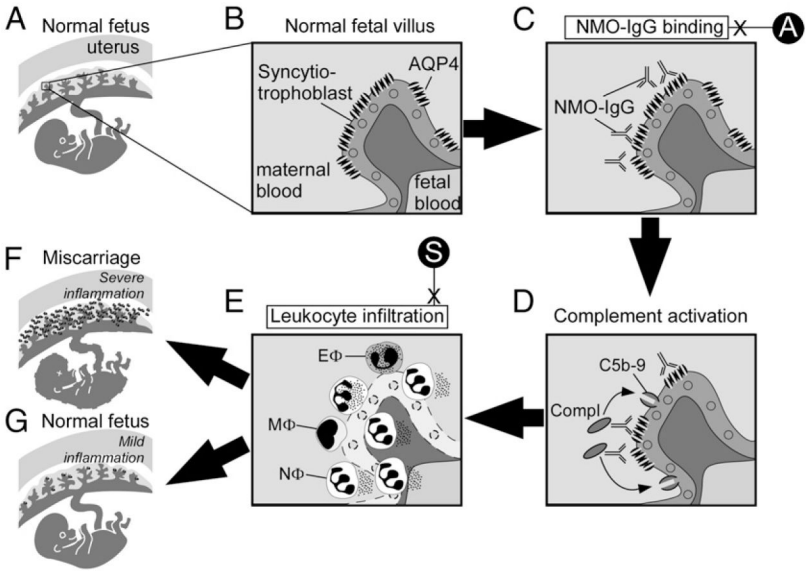

FIGURE 5.

Proposed mechanism of NMO-IgG–induced placental inflammation. **(A**) Normal fetus in uterus with a (**B**) magnified view of a normal fetal villus showing AQP4 within the syncytiotrophoblast plasma cell membrane. (**C**) NMO-IgG binds extracellular epitopes on AQP4 and (**D**) activates complement causing the deposition of membrane attack complexes (C5b-9) in the syncytiotrophoblast plasma membrane. (**E**) Leukocytes infiltrate the placenta, primarily neutrophils (NΦ) with some eosinophils (EΦ) and macrophages (MΦ). (**F**) Severe placental inflammation causes fetal death, but (**G**) mild placental inflammation allows normal fetal growth. Aquaporumab (A) inhibits NMO-IgG binding, and sivelestat (S) inhibits neutrophil-mediated damage.